Title: Unveiling lipid chemodiversity in root exudates: A comprehensive characterization of the exudate metabo-lipidome in Tall Wheatgrass

Sneha P. Couvillion[1] (0000-0003-0307-9343), Isabella H. Yang[1] (0000-0002-1490-3329), Josie Eder[1] (0000-0002-2876-0496), Sheryl Bell[1] (0000-0001-8445-1375), Kirsten S. Hofmockel[1,*] (0000-0003-1586-2167)

[1]Earth and Biological Sciences Directorate, Pacific Northwest National Laboratory, Richland, WA, USA

*Corresponding author: kirsten.hofmockel@pnnl.gov

Keywords: metabo-lipidomics, root exudates, lipids, mass-spectrometry, tall wheatgrass, metabolite annotation, rhizodeposition, molecular chemodiversity

Abstract

The rhizosphere, where plant roots meet soil, is a hub of biogeochemical activity with ecosystem impacts on carbon stocks (Hopkins *et al.*, 2013). Root derived carbon has been found to contribute more to soil carbon stocks than aboveground litter (Austin *et al.*, 2017), but the molecular chemodiversity of root exudates remains poorly understood. Here our goal was to discover the molecular chemodiversity of metabolites and lipids in root exudates to advance our understanding of plant root inputs belowground. We worked with mature, field-grown tall wheatgrass (*Thinopyrum ponticum*) and optimized exudate collection protocols to enable the capture of non-polar lipids in addition to polar and semi-polar metabolites. We found that rates of C input via hydrophobic exudates were approximately double that of aqueous exudates and C/N ratios were markedly higher in hydrophobic compared to aqueous exudates, emphasizing the importance of lipids, due to their high carbon content. We used liquid chromatography coupled tandem mass-spectrometry for paired untargeted metabolomics and lipidomics or 'metabo-lipidomics' for maximizing molecular coverage. To address the challenge of metabolite annotation, we employed both MS/MS spectral library searching and deep learning-based

chemical class assignment, substantially increased the characterization of the chemodiversity of root exudates. Notably, in an unprecedented characterization of intact lipids in root exudates, we discovered the presence of a diverse variety of lipids, including substantial levels of triacylglycerols (~19 µg/g fresh root per min), fatty acyls, sphingolipids, sterol lipids, and glycerophospholipids. Thus our study offers novel insights into the chemodiversity of lipids, positioning them as significant carbon inputs in root exudates.

Introduction

Root Exudates: Major Carbon Inputs and Regulators of Soil Organic Matter (SOM) Dynamics

Current estimates of direct plant contributions to SOM pools such as mineral associated organic matter (MAOM) are likely undervalued given the reliance on aboveground plant tissue proxies for determining plant and microbial origin (Whalen *et al.*, 2022). The roles of small molecule metabolites, especially lipids, in shaping interkingdom interactions and microbial processes that control cycling and long-term storage of carbon are poorly understood. Metabolites and lipids play diverse roles in regulatory, metabolic, and signaling networks among microbes and in microbe-plant interactions and are sensitive indicators of organismal phenotypes and community metaphenomes (Jansson & Hofmockel, 2018). However, challenges in identifying key molecules and elucidating their functions are critical frontiers in soil ecosystem research.

Plants carry out the necessary first step of siphoning atmospheric carbon into soil through photosynthesis. It is estimated that 5-40% of photosynthetically fixed carbon enters soil through root exudation (BADRI & VIVANCO, 2009; Simon & Haichar, 2019). Exudates regulate SOM dynamics by contributing to SOM stabilization and turnover. Small molecules in root exudates, such as lipids, function as both signaling compounds and microbial nutrients that shape the assembly and activity of microbial communities (Mark *et al.*, 2005; Hugoni *et al.*, 2018; Sasse *et al.*, 2018; Zhalnina *et al.*, 2018; Huang *et al.*, 2019). They influence the colonization, growth, and activity of key microbial members including mycorrhizal fungi (Elias & Safir, 1987; Tian *et al.*, 2021), impact soil physical structure (Naveed *et al.*, 2017), induce soil respiration (de Vries *et al.*,

2019) and can cause priming, decomposition, and mineralization of SOM. These small molecules may regulate microbial metabolism, undergo assimilation into microbial biomass, transformation by extracellular enzymes, or association with soil minerals, ultimately integrating into SOM. Research on exudate-induced priming (Fontaine *et al.*, 2007; Chen *et al.*, 2019) and factors controlling the formation of stable SOM (Kallenbach *et al.*, 2016; Liang *et al.*, 2023) have predominantly used single or simplistic exudate surrogates such as glucose, cellulose and cellobiose. However, this approach overlooks the realistic chemodiversity present in exudates. By relying on these surrogates, the studies tend to simplify plant inputs to carbon sources alone, neglecting the diverse metabolic, regulatory, and signaling roles played by the small molecules present in exudates. Different chemical classes of root exudate surrogates induce distinctly different magnitudes of priming and these effects are likely non-additive in complex mixtures, emphasizing the complexity of their effects on SOM stocks (Yan *et al.*, 2023). A recent long-term study suggests that root-derived inputs lead to net SOM gains after initial priming, emphasizing the need to consider root exudate molecular complexity and ecologically relevant timescales (Schiedung *et al.*, 2023).

Capturing Exudate Chemodiversity using Metabo-Lipidomics: Navigating Beyond just Sugars and Organic Acids into the Uncharted Territory of Lipids

Recent studies using liquid chromatography coupled with mass spectrometry (LC-MS/MS) for untargeted metabolomics have revealed a broad spectrum of polar and semi-polar small molecules in exudates (Dietz *et al.*, 2019; McLaughlin *et al.*, 2023). While progress has been achieved in characterizing these metabolites, the comprehensive identification of the numerous features detected by mass spectrometry remains a significant bottleneck in metabolomics, with only a small fraction of features being currently identified (da Silva *et al.*, 2015). Importantly, the exploration of lipids, a crucial group of non-polar metabolites, is notably absent in exudate studies. Their distinctive hydrophobic properties present challenges in detection and analysis using conventional methods for exudate collection and analysis. Our recent work demonstrates the value of intact lipids in soil ecosystems as sensitive indicators of environmental stress

response and substrate availability and highlights their great potential for interrogating interkingdom interactions and resource sharing (Couvillion *et al.*, 2023; Naasko *et al.*, 2023).

In this study, we hypothesized that plant roots exude a diverse array of intact lipids, potentially serving as microbial energy sources, chemotactic signals, antimicrobial compounds, and metabolic regulators in the rhizosphere. Accurately assessing plant exudate profiles, which are significantly influenced by growth stage and growth conditions, requires collecting root exudates from mature plants in a way that realistically recapitulates natural field conditions (Dietz *et al.*, 2019; Williams *et al.*, 2021). This was highlighted by a recent study which found higher total carbon in hydroponic exudates, whereas field-grown plant exudates contained more secondary metabolites- suggesting hydroponic root exudates may not fully capture the exudate composition and chemodiversity of field environments (Heuermann *et al.*, 2023). We chose to work with mature, field grown tall wheatgrass plants (*Thinopyrum ponticum*, cultivar: Alkar) to maximize translation to perennial plants in the field. To collect the full diversity of small molecules, we optimized exudate collection protocols to enable the capture of non-polar lipids in addition to polar and semi-polar metabolites. We found that C and N input rates in hydrophilic and hydrophobic exudates were 38.41 $\pm$ 5.93 and 81.52 $\pm$ 13.81 μg C g^{-1} fresh root mass min^{-1}, respectively, and 2.68$\pm$ 0.42 and 0.20 $\pm$ .04 μg N g^{-1} fresh root mass min^{-1}, respectively. The C/N of hydrophilic exudates was far lower than that of hydrophobic exudates (14.40 $\pm$ 0.58 vs 459 $\pm$ 90), which is consistent with high C content in lipids. We used liquid chromatography coupled tandem mass-spectrometry (LC-MS/MS) for paired untargeted metabolomics and lipidomics or 'metabo-lipidomics' (**Fig. 1A**); we employed three liquid chromatography column chemistries and analyzed samples in positive and negative ionization modes for maximizing coverage of the metabo-lipidome. Additional details on the methods can be found in the 'Methods and Materials' section. The results from the metabolomics and lipidomics analyses will be discussed separately.

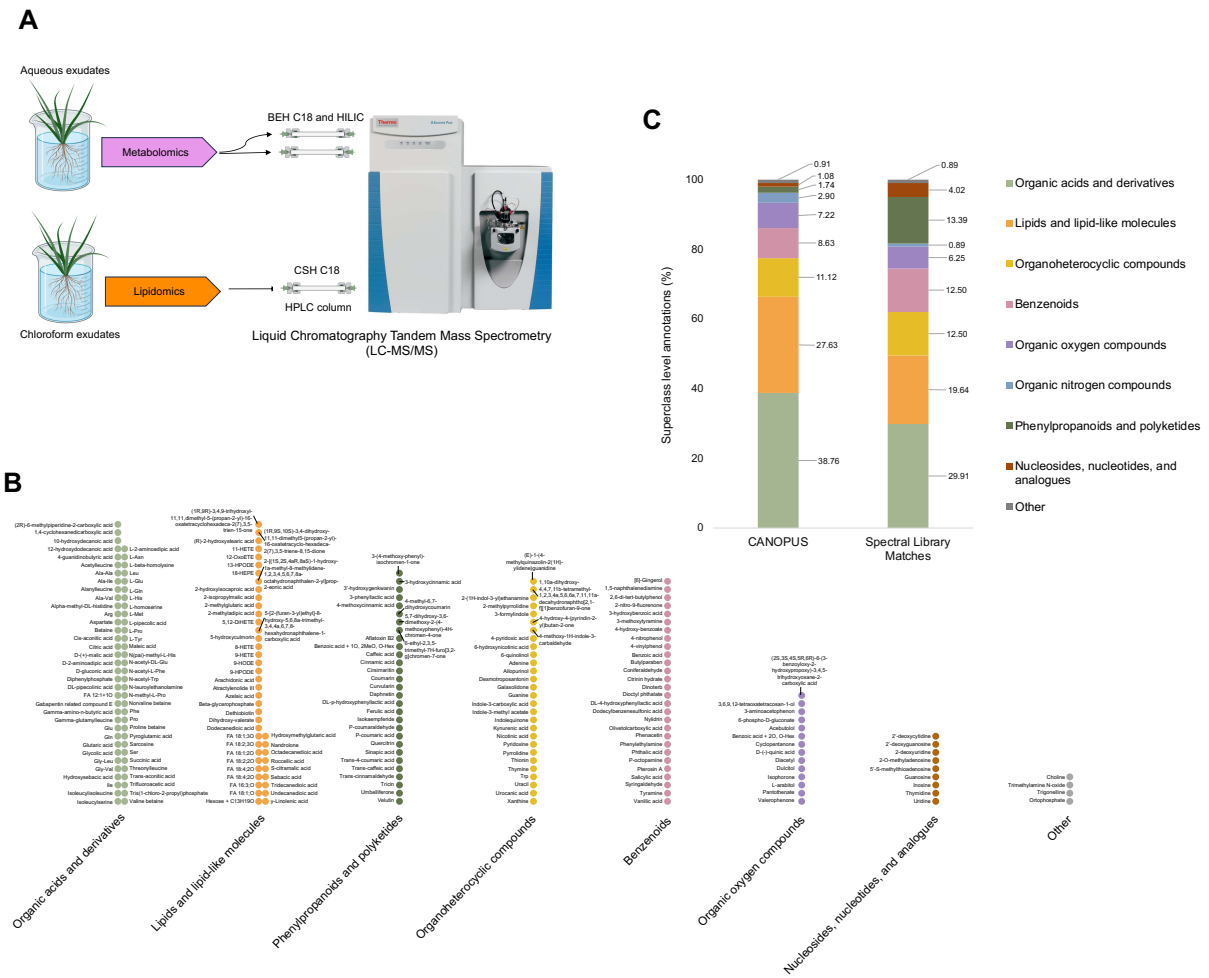

Figure 1: A) Untargeted LC-MS/MS based metabo-lipidomics workflow; B) Metabolites annotated using spectral library searching, colored and listed by superclass C) Percent distribution of superclass level classification of metabolomics features annotated using CANOPUS and spectral library searching (SLS)

Tackling the Unknowns: Enhancing Metabolite Annotation and Classification by Combining Spectral Library Searching with CANOPUS

Metabolite identification in mass-spectrometry analyses poses a major challenge in metabolomics research (Monge *et al.*, 2019). To address this, our study combines two strategies for improved feature annotation. We employed spectral library searching (SLS) to assign annotations to 224 unique metabolites (Schymanski confidence level 2A (Schymanski *et al.*, 2014), **Fig 1B**), using in-house and publicly available MS/MS databases. These annotations were

established through accurate mass and tandem mass spectra matching, with additional consideration of retention time when there was a match to the in-house library. Using the SLS approach we identified 67 metabolites belonging to the 'Organic acids and derivatives' superclass, primarily comprising amino acids and analogues, and dipeptides. The ‘Lipids and lipid-like molecules’ superclass ranked second, encompassing 44 metabolites, predominantly composed of fatty acids, derivatives, and prenol lipids. The 'Phenylpropanoids and polyketides' superclass contained 30 metabolites, including cinnamic acids and derivatives, flavonoids, coumarins, phenylpropanoic acids, and cinnamaldehydes. Similarly, the superclasses 'Organoheterocyclic compounds' (indoles, pyridines, quinolines, and derivatives) and 'Benzenoids' (benzene derivatives, phenols) each comprised 28 metabolites. Finally, the superclasses 'Organic Oxygen Compounds' and 'Nucleosides, nucleotides, and analogues' contained 14 and 9 metabolites, respectively.

These finding show that field grown tall wheatgrass root exudates contain a rich diversity of metabolites spanning various superclasses, some of which are recognized for their roles in mediating stress responses, plant-microbe interactions, nutrient cycling, and defense mechanisms. In addition to primary metabolites, we identified a diverse array of secondary metabolites including benzoic acid derivatives, prenol lipids, indoles and derivatives, cinnamic acids, coumarins and flavonoids. Metabolites belonging to these subclasses have been shown to have a role in plant defense, stress response, microbial recruitment, and signaling pathways (Van Poecke *et al.*, 2001; Zhang *et al.*, 2009; Hassan & Mathesius, 2012; Schenkel *et al.*, 2015; Massalha *et al.*, 2017; Tian *et al.*, 2021). Among the 224 metabolites that we identified through spectral library matching, we found that 43 have been previously reported (Strehmel *et al.*, 2014; Zhalnina *et al.*, 2018; McLaughlin *et al.*, 2023) in root exudate characterizations of other plants. Notably, 30 of these metabolites were recently characterized as part of the core exudate metabolome (McLaughlin *et al.*, 2023) in three model plants—*Arabidopsis thaliana, Brachypodium distachyon*, and *Medicago truncatula*—constituting 40% of the 75-molecule core exudate metabolome. The shared compounds prominently featured nucleobases (adenine, guanine, thymine, uracil) and organic acids, particularly amino acids (asparagine, glutamic acid, glutamine, histidine, leucine,

150 proline, tyrosine), indicating a commonality of these small molecules in exudates across diverse
151 plant species.
152
153 While database-dependent methods such as SLS, offer valuable insights into chemical structures,
154 their identification rate is constrained by the library's scope, leaving a substantial majority- often
155 ~90%- of features unannotated (da Silva *et al.*, 2015). This is a central challenge in the field of
156 metabolomics that needs to be addressed in order to obtain ecological insights from molecular
157 level data (Peters *et al.*, 2018). To maximize the biological information obtained from the
158 unannotated features which are typically discarded from downstream analyses, we
159 complemented SLS with CANOPUS (Dührkop *et al.*, 2021), a deep learning-based class assignment
160 and ontology prediction tool, to predict chemical classifications for 1559 detected, high quality
161 features. It's important to note that due to the higher masses of many lipids, CANOPUS analysis
162 was exclusively applied to the metabolomics data. CANOPUS predicted classifications for 80% of
163 these features spanning 12 superclasses (1205 features classified), 56 classes (1084 features), 85
164 subclasses (822 features), and 60 level 5 classifications (588 features). Approximately 1250
165 features received at least one level of classification, substantially increasing our characterization
166 of the chemodiversity of plant exudates. The SLS and CANOPUS analyses uses two separate
167 software (MS-DIAL and MZmine) for feature detection and alignment; it wasn’t possible to match
168 features across the analyses.
169
170 The superclass-level distribution of annotations from spectral library search (SLS; 224 features)
171 and CANOPUS (1205 features) exhibited similar trends (**Fig 1C**). 'Organic acids and derivatives'
172 predominated in both approaches (SLS 30%, CANOPUS 39%), comprising mainly amino acids,
173 derivatives, and peptides. Following closely was the 'Lipid and lipid-like molecules' superclass (SLS
174 20%, CANOPUS 28%), where fatty acids and conjugates were prominent. 'Organoheterocyclic
175 compounds' (SLS 12.5%, CANOPUS 11%), 'Benzenoids' (SLS 12.5%, CANOPUS 9%), 'Organic
176 oxygen compounds' (SLS 6%, CANOPUS 7%), including carbohydrates and carbonyl compounds,
177 'Organic nitrogen compounds' (SLS 1%, CANOPUS 3%), 'Phenylpropanoids and polyketides' (SLS

178 13%, CANOPUS 2%), and 'Nucleosides, nucleotides, and analogues' (SLS 4%, CANOPUS 1%)
179 followed.
180
181 **Discovering the Diversity of Lipids in Root Exudates**
182 In the untargeted lipidomics data, 7864 features with MS/MS spectra were detected in positive
183 and negative ionization modes combined. Of these, 289 (~4%) lipid features (including isomers)
184 comprising 267 unique InChIKeys(Heller *et al.*, 2015) were annotated using MS/MS database
185 matching (Schymanski identification confidence level 2A (Schymanski *et al.*, 2014)) with MS-DIAL.
186 Lipids from the glycerolipid and fatty acyl categories were particularly prevalent, followed by
187 sphingolipids, sterol lipids, and glycerophospholipids [**Fig. 2A**]. Known functions of these lipids
188 include diverse roles in membrane structure and stability, energy storage, cell signaling and
189 responses to stress.
190 In hydrophobic root exudates of mature tall wheatgrass, we found that glycerolipids, particularly
191 triacylglycerols (TG), represent a dominant fraction, comprising 47% of the lipidome. Subclass
192 analysis reveals the prevalence of triradylglycerols (TG), diradylglycerols (DG), and
193 monoradylglycerols (MG) at 33%, 12%, and 2% of annotated lipids, respectively.
194 We examined the distribution of fatty acids within the glycerolipids to identify the top three
195 predominant fatty acids—16:1, 16:0, and 18:1—followed by 18:2, 20:4, 20:5, 20:3, and 24:1,
196 shaping the composition of TG, DG, and MG in root exudates (**Fig 2B**). To approximately quantify
197 glycerolipids in exudates, we spiked a deuterated standard for each subclass. During a 5-minute
198 hydrophobic exudate collection, roots exuded 2 µg of MG, 17.2 µg of DG, and 95.1 µg of TG per
199 gram of fresh root mass. Extrapolating this rate suggests a noteworthy daily exudation of
200 approximately 806 mg of TGs per plant. It is worth noting that there can be diurnal variations
201 (McLaughlin *et al.*, 2023) in exudation rates and the hydrophobic exudate collection protocol,
202 involving a 5-minute immersion in chloroform, may induce stress on plant roots which could
203 impact TG metabolism and exudation rates, given the role of TGs in protecting against oxidative
204 stress (Fan *et al.*, 2017). Further investigation into these potential influences is necessary. The
205 specific roles of glycerolipids in exudates remain unclear, necessitating systematic investigations
206 in subsequent studies. We propose that these lipids may influence microbial dynamics, serving as

A

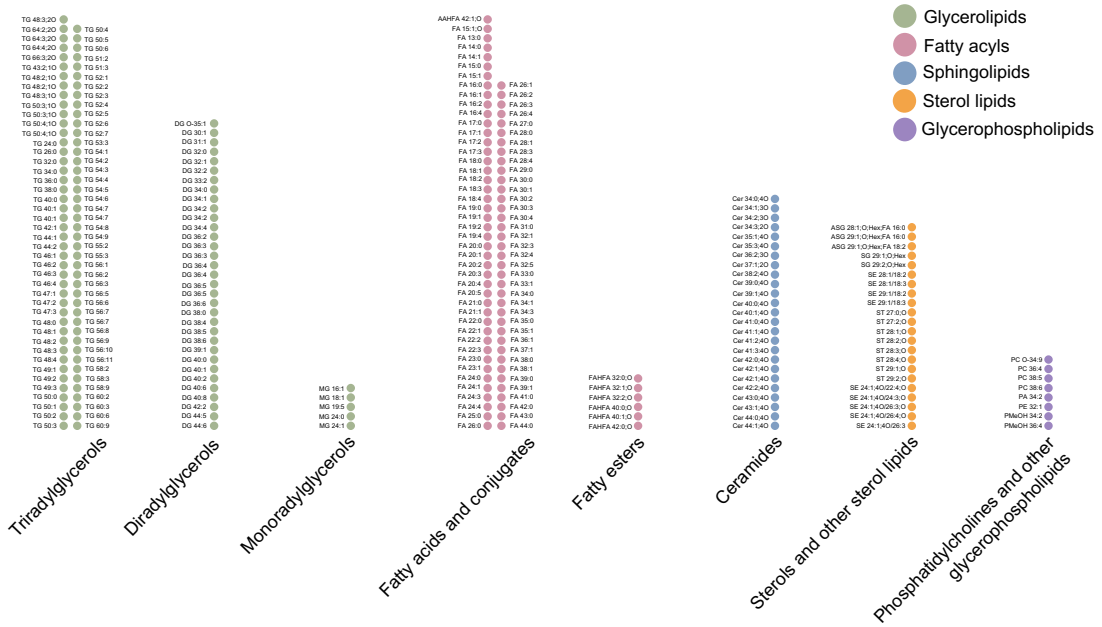

B

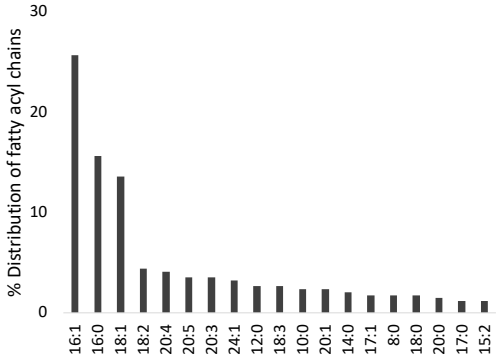

Figure 2: A) Level 2A feature annotations in untargeted lipidomics data; grouped and colored by lipid main class B) Distribution of fatty acid residues in glycerolipids

a nutrient source, fostering symbiotic relationships, and impacting the formation and stabilization of water-stable aggregates. Breakdown lipids such as triacylglycerols require extracellular microbial enzymes including esterases and lipases and studies suggest that these lipids may persist longer than simple sugars in soil (Soliman & Radwan, 1981; Hita *et al.*, 1996).

212 Amongst the fatty acyl category, 30% of the identified lipids belonged to the subclass of free fatty
213 acids (FA). Fatty acids and derivatives are known to carry out important functions such as
214 stimulating P-solubilizing activity (Pantigoso *et al.*, 2023) and denitrification activity (Lu *et al.*,
215 2014) in rhizosphere bacteria as well as sustaining AMF germination and sporulation (Kameoka &
216 Gutjahr, 2022). However, given the sparse tandem mass spectral fragmentation of FAs, future
217 work needs to confirm the identity of FAs using standards for retention time confirmation and/or
218 gas chromatography coupled with mass spectrometry. Aside from FAs, the remaining fatty acyls
219 consisted of six fatty acyl esters of hydroxy fatty acids (FAHFAs) and one acyl alpha-hydroxy fatty
220 acid (AAHFA). FAHFAs are a recently discovered class of bioactive lipids found in plants, yeast and
221 mammals, some of which exhibit anti-inflammatory and anti-diabetic activity (Yore *et al.*, 2014;
222 Kolar *et al.*, 2019). The role of these lipids in root exudates is still unknown.
223
224 Sphingolipids—specifically ceramides—made up 9% of the annotated lipids [**Fig. 2A**]. Ceramides
225 serve many functions in plants, including cell signaling, stress response, and membrane integrity.
226 The biophysical properties and functions of ceramides can vary depending on the constituent
227 sphingoid base and fatty acid. The ceramides we detected were largely composed of trihydroxy
228 long chain bases (LCB) 18:0 and 18:1 (48% and 16% of the ceramides respectively), and α-hydroxy
229 fatty acids varying in length from 16 to 26 carbons which are typical in plants (Lynch & Dunn,
230 2004). Isolated LCBs have been shown to inhibit the growth of plant-associated fungi and bacteria
231 *(Glenz et al., 2022).* Ceramides in other host-microbe ecosystems such as human skin are known
232 to inhibit pathogenic biofilm formation (Cleary *et al.*, 2018). The functions of ceramides in root
233 exudates are yet to be elucidated, but their potential roles in regulating the growth of plant-
234 associated microbes and biofilms warrant further investigation given their abundance in root
235 exudates.
236
237 Phytosterols, accounting for 8% of identified lipids, play key roles in plant-microbe interactions
238 and plant health. We identified stigmasterol, a plant sterol with demonstrated potential for
239 improving nitrogen use efficiency in the rhizosphere. A recent study revealed that a denitrifying
240 bacterial inoculant strain could influence stigmasterol concentrations in duckweed root exudates

241 leading to increased nitrite reductase activity, biofilm formation, and promotion of plant growth
242 (Lu *et al.*, 2021). Only eight glycerophospholipids (3%) were identified and these included
243 phosphatidylcholines and phosphatidylethanolamine which are abundant phospholipids in plant
244 cell membranes. The low number of phospholipids detected suggests that the hydrophobic
245 exudate collection protocol used in this study effectively captured lipids arising from root
246 exudates rather than from root cell membranes or surface attached microbial cells.
247
248 **Conclusions and future directions**
249 A comprehensive characterization of small molecules-including lipids-in root exudates is a critical
250 first step for advancing our understanding of the functions and fate of rhizodeposites in terrestrial
251 ecosystems. Using mature, field-grown tall wheatgrass plants as a case study, we demonstrate
252 the first comprehensive characterization of the root exudate metabo-lipidome. We found that C
253 input rates in hydrophobic exudates were around double that of aqueous exudates and C/N ratios
254 were markedly higher in hydrophobic exudates when compared to aqueous (459 ± 90 vs 14.40 ±
255 0.58). Despite the caveat that there may be variations in exudation in undisturbed soil
256 environments and our collection methods that use water and chloroform, these findings
257 emphasize the need to pay closer attention to the lipid fraction of root exudates and highlight the
258 need to investigate the impact of exudate lipids on microbial physiology, carbon use efficiency,
259 and SOM formation and turnover. In an unprecedented characterization of intact lipids in root
260 exudates, our results reveal the presence of a variety of lipids with diverse functions, with
261 substantial levels of triacylglycerols which previously were not known to be exuded by roots. The
262 combined use of SLS and CANOPUS strategies for metabolite identification, not only enabled high
263 confidence annotations via spectral library searches but also facilitated a broader assignment of
264 chemical class information across detected features. This dual strategy, leveraging the strengths
265 of both methods, enhanced the depth and coverage of metabolite identification, contributing to
266 a more thorough understanding of the exudate metabolome. Overall, with 513 metabolite and
267 lipid identifications and chemical classification of 1250 features (~80% of all high-quality features
268 detected), this work represents the most comprehensive molecular characterization of root
269 exudates so far.

Achieving sustainable and climate-focused ecosystems requires an understanding of the impact of root exudates on microbial community functions and soil carbon dynamics. The findings in this work will be critical in resolving current uncertainties in quantifying plant contributions to SOM formation and stabilization. Future studies need to quantify the impacts of environmental factors (climate, soil properties) on the exudate metabo-lipidome, and evaluate the functional consequences of various small molecules on microbial metabolism and activity. Leveraging the findings in this work, targeted incubations with exudate metabolites and lipids can be designed to understand the effect of these molecules on microbial metabolism and their interactions with minerals. The impact and contributions of root endophytes and symbionts such as arbuscular mycorrhizal fungi on exudate chemistry is not known and warrants interrogation. Investigations on priming can incorporate increasingly complex mixtures or natural exudates to understand microbial community responses in realistic conditions. Comprehensive molecular mapping of the soil metabo-lipidome, by systematic characterization of small molecule metabolites and lipids from plant and microbial sources, and their cross-feeding between organisms, is essential for understanding interactions and metabolic pathways that drive ecological functions such as SOM formation and nutrient cycling.

As we navigate the open frontier of exploring the functions of lipids in root exudates and soil ecosystems, particularly their potential to enhance plant health, long-term storage of soil carbon and ecosystem resilience, the identification of key bioactive exudate metabolites and lipids becomes paramount. This knowledge can inform breeding of desired plant traits to facilitate plant-microbe partnerships that can enhance plant productivity and stress tolerance, all while promoting soil carbon storage. In essence, understanding the complex interplay between lipids in root exudates and soil microbial communities provides valuable insights for sustainable agricultural practices and biofeedstock ecosystem management.

298 **Methods**

299

300 **Plant harvest and exudate collection**:

301 Five mature tall wheatgrass (*Thinopyrum ponticum*, cultivar: Alkar) plant bunches were harvested
302 in October 2022 from our Tall Wheatgrass Field Trial site at Washington State University (WSU)-
303 Irrigated Agriculture Research and Extension Center (WSU-IAREC) in Prosser, WA, USA. These
304 plants were established in 2018 and were allowed to grow for ~4 years under normal irrigation
305 conditions. Plants were harvested along with their intact roots and the surrounding soil using a
306 shovel to unearth a root ball that was approximately 30 cm wide x 30 cm deep. After gentle
307 removal of root-associated soil, plant roots were washed in MilliQ water by submerging and
308 shaking gently to remove any remaining soil. After washing, the plants were transferred to 5 L
309 glass beakers where their roots were submerged in 1.5 L of pure milliQ water for 2 hours. The
310 aqueous exudate solutions were vacuum filtered at 0.22 µm and aliquoted into 50 mL tubes for
311 storage at -80 C. Subsequently, the plants roots were transferred to 5 L glass beakers where their
312 roots were submerged in 500 mL chloroform for 5 minutes to collect hydrophobic lipids in
313 exudates. The chloroform exudates were aliquoted into 50 mL tubes for storage at -80 C. 25 mL
314 of aqueous or chloroform exudates were vacuum dried and reconstituted for downstream
315 metabolomics and lipidomics analysis respectively.

316

317 **Mass spectrometry (LC-MS/MS) analysis**:

318 Metabolites were analyzed using reverse phase (RP) and hydrophilic interaction chromatography
319 (HILIC) separations on a Thermo Fisher Scientific HF-X mass spectrometer (Thermo Scientific, San
320 Jose, CA) coupled with a Waters Acquity UPLC H class liquid chromatography system (Waters
321 Corp., Milford, MA). Metabolites were brought up in 200 uL of 50% LCMS grade methanol and
322 50% nanopure water. RP separation was performed by injecting 5 uL of sample onto a Thermo
323 Scientific Hypersil GOLD C18 column (3 µm, 2.1 mm ID X 150 mm L) heated to 40°C. Metabolites
324 were separated using an 18 minute gradient with data collected on the first 17 minutes. The RP
325 mobile phase A consisted of 0.1% formic acid in nanopure water and a mobile phase B consisting
326 of 0.1% formic acid in LCMS grade acetonitrile. The gradient used was as follows (min, flowrate in

327 mL/min, %B): 0,0.4,10; 2,0.4,10; 11,0.4,90; 12,0.4,90; 12.5,0.5,90; 13.5,0.5,10; 14,0.5,10;
328 14.5,0.4,10; 15,0.4,10. Positive and negative ion modes were analyzed in separate injections.
329 HILIC separation was performed by injecting 3 uL of sample onto a Waters Acquity BEH Amide
330 column (130 Å, 1.7 µm, 2.1 mm ID X 100 mm L) heated to 55°C. Metabolites were separated
331 using a 16 minute gradient with data collected for the first 15 minutes. The HILIC mobile phase A
332 consisted of 0.05% ammonium hydroxide, 5% LCMS grade acetonitrile, and 94.95% 10 mM
333 ammonium acetate in nanopure water with a mobile phase B consisting of 0.05% ammonium
334 hydroxide in 99.95% LCMS grade acetonitrile. The gradient used was as follows (min, flowrate in
335 mL/min, %B): 0,0.3,95; 6,0.3,37; 7,0.3,37; 7.1,0.3,95; 7.2,0.5,95; 9.5,0.5,95; 9.7,0.3,95; 16,0.3,95.
336 Positive and negative ion modes were analyzed in separate injections. For both RP and HILIC
337 separations the Thermo Fisher Scientific HF-X was equipped with a HESI source and high flow
338 needle with the following parameters: spray voltage of 3.6 kV in positive mode and 3kV in
339 negative mode, capillary temperature of 300°C, probe heater temp of 370°C, sheath gas at 60
340 L/min, auxiliary gas at 25 L/min, and spare gas at 2 L/min. Metabolites were analyzed at a
341 resolution of 60 k and a scan range of 50 to 750 m/z for parent ions followed by MS/MS HCD
342 fragmentation which is data dependent on the top 4 ions with a resolution of 15 K and stepped
343 normalized collision energies of 20, 30, and 40. Total organic carbon (TOC) and total nitrogen (TN)
344 in metabolite extracts were measured in acidified extracts on a Vario TOC cube (Elementar,
345 Germany). C/N ratio was calculated by the ratio of TOC and TN.

346 Lipid extracts were analyzed by RP separation using a Waters Aquity UPLC H class system
347 (Waters Corp., Milford, MA) coupled with a LTQ Velos Elite Orbitrap mass spectrometer (Thermo
348 Scientific, San Jose, CA). Samples were stored in 2 parts chloroform and 1 part methanol, were
349 evaporated, and reconstituted in 100 µL of 90% methanol and 10% chloroform prior to injecting
350 10 µl onto a Waters column (CSH 3.0 mm x 150 mm x 1.7 µm particle size) heated to 42°C. Lipids
351 were then separated using a 42 min gradient with data collected on the first 34 minutes. Mobile
352 phase A consisted of 10mM ammonium acetate in 60% nanopure water and 40% LCMS grade
353 acetonitrile with a mobile phase B consisting of 10 mM ammonium acetate in 90% LCMS grade
354 isopropanol and 10% LCMS grade acetonitrile. The gradient used for both positive and negative
355 mode was as follows (min, flowrate, %B): 0,0.25,40; 2,0.25,50; 3,0.25,60; 12,0.25,70; 15,0.25,75;

356 17,0.25,78, 19,0.25,85; 22,0.25,92; 25,0.25,99; 34,0.25,99; 34.5,0.3,99; 35,0.3,99; 35.5,0.3,99;
357 36,0.35,40; 37,0.3,40; 38,0.25,40. A Thermo HESI source was coupled to the mass spectrometer
358 inlet with both heated to 350°C with a spray voltage of 3.5 kV and sheath, auxiliary, and sweep
359 gas flows of 45, 30, and 2, respectively. Positive and negative polarities were analyzed in separate
360 sample runs. Lipids were fragmented by both HCD and CID using a parent ion scan of 200-2000
361 m/z with a 60 k resolving power. Subsequent MS/MS was performed on the top 4 ions. An
362 isolation width of 2 m/z units and a maximum charge state of 2 were used for both CID and HCD
363 scans. A normalized collision energy of 35 was used for CID while 30 was used for HCD. CID spectra
364 were acquired in the ion trap using an activation Q value of 0.18, while HCD spectra were acquired
365 in the Orbitrap at a mass resolution of 7.5 k and a first fixed mass of m/z 90. For quantification of
366 glycerolipids, a sample was spiked with EquiSPLASH lipid mix (Avanti Polar Lipids) containing
367 deuterated TG, DG and MG internal standards and run in positive and negative mode with each
368 injection containing 0.1 µg of each standard. The area under the peak for the standards was used
369 for quantifying the total amount of lipids of the same lipid class in the samples. Total carbon (TC)
370 and nitrogen (TN) content in lipid extracts was quantified after drying down extracts in tin
371 capsules by using an Elementar Vario Isotope cube elemental analyzer (Elementar, Germany). C/N
372 ratio was calculated by the ratio of TC and TN. Chloroform blanks were analyzed alongside
373 samples to control for residual C contributed by the solvent.
374
375 Data processing: Metabolite and lipid identifications were made using MS-DIAL v4.92 for peak
376 detection, identification and alignment. For metabolomics, the experimental data was matched
377 both to in-house libraries (m/z less than 0.003 Da, retention time less than 0.3 min, MS/MS
378 spectral match) and a compilation of publicly available MS/MS databases (m/z less than 0.003 Da,
379 MS/MS spectral match) (VS17) available in the MS-DIAL metabolomics MSP spectral kit
380 (http://prime.psc.riken.jp/compms/msdial/main.html#MSP). The tandem mass spectra and
381 corresponding fragment ions, mass measurement error, and aligned chromatographic features
382 were manually examined to remove false positives. Relative quantification was performed by
383 calculating peak areas on extracted ion chromatograms of precursor masses. Features detected
384 in at least three of the five replicates were retained.

385

386 Although confident structural identification of features remains a central goal of metabolomics
387 and lipidomics, it is useful to note that a considerable fraction of features detected in untargeted
388 mass-spectrometry based analyses can arise due to artifacts such as in-source fragments,
389 adducts, isotopes, and contaminants and may not all be biological, unique or informative (Peisl
390 *et al.*, 2018). To prepare metabolomics data for CANOPUS analysis, Proteowizard (Chambers *et*
391 *al.*, 2012) and MZmine3 (Schmid *et al.*, 2023) were used on each mode separately. Raw data was
392 centroided, peak-picked, and converted to compatible formats with Proteowizard. Resulting
393 mzML files were imported into MZmine3 and underwent noise cancellation and automated data
394 analysis pipeline (ADAP) chromatogram generation. Noise intensity levels were set at 6.0E3–8.0E3
395 a.u. (arbitrary units) for MS2 spectra and 6.0E4–1.0E5 a.u. for MS1. The local minimum resolver
396 was manually adjusted to reduce peak broadening and splitting; only significant peaks in the
397 chromatograms were recognized as features. Minimum absolute peak height was set to 1.5E5–
398 2.5E5 a.u. across the modes. 13C related peaks within the same feature list were removed such
399 that only the most significant isotope remained. The isotope pattern finder was also used to
400 detect stable isotopes of hydrogen, carbon, nitrogen, oxygen, sulfur, and phosphorus. Deisotoped
401 feature lists were aligned to produce one feature list with data from the entire mode. Further
402 analysis filtered out rows with less than two features present and remaining ^{13}C isotopes. Finally,
403 as feature detection steps (e.g. peak height below minimum intensity, alignment errors, etc.) may
404 result in lost peaks, gap filling was performed. The resulting aligned, filtered, and gap-filled
405 feature list of each mode was exported as an MGF file. Molecular networking files were saved for
406 downstream analysis. A total of 1559 high quality features with MS2 scans were obtained across
407 the 4 modes.

408

409 MGF files were transferred to SIRIUS 5.7.2. (Duhrkop *et al.*, 2019) for CANOPUS analysis.
410 CANOPUS utilized the fragmentation trees and molecular fingerprints to predict ClassyFire
411 classifications of features (Djoumbou Feunang *et al.*, 2016; Duhrkop *et al.*, 2021). Classifications
412 with certainties/confidence below 75% were discarded. Summaries were exported with
413 CANOPUS ClassyFire predictions.

Funding and Acknowledgements

PNNL is a multi-program national laboratory operated by Battelle for the DOE under Contract DE-AC05-76RLO 1830. This program is supported by the U. S. Department of Energy, Office of Science, through the Genomic Science Program, Office of Biological and Environmental Research, under FWP 70880. A portion of this work was performed in the William R. Wiley Environmental Molecular Sciences Laboratory (EMSL), a national scientific user facility sponsored by the Office of Biological and Environmental Research and located at PNNL. IY was supported by the DOE SULI internship program. The authors thank Jayde Aufrecht, Daisy Herrera, Sharon Zhao, Eric Garza, Meagan Burnet and Jesse Trejo for assisting with root exudate sample collection following the plant harvest, Sophia McKever and Kaizad Patel for assistance with TC/TN measurements and Shannon Sheridan for helping curate the data package on DataHub.

Author Contributions

SPC conceived the initial idea and SPC and KSH designed the study. SPC and SLB carried out field collection of plants and exudates. SLB measured TC and TN content in samples. JE collected the LC-MS/MS data on the instrument and helped with glycerolipid quantification. SPC and IY analyzed the metabolomics and lipidomics data and wrote the initial draft of the manuscript. All authors contributed to produce the final draft. KSH obtained the funding.

Data Availability

Primary raw mass spectrometry lipidomics and metabolomics data have been deposited at MassIVE under the accession: MSV000093600 (will be made public after peer-review when manuscript is accepted for publication).

Competing interest statement: The authors declare that they have no known conflicts of interest or competing financial interests that influence this work.

References

Austin EE, Wickings K, McDaniel MD, Robertson GP, Grandy AS. 2017. Cover crop root contributions to soil carbon in a no-till corn bioenergy cropping system. *GCB Bioenergy* 9(7): 1252-1263.

BADRI DV, VIVANCO JM. 2009. Regulation and function of root exudates. *Plant, Cell & Environment* 32(6): 666-681.

Chambers MC, Maclean B, Burke R, Amodei D, Ruderman DL, Neumann S, Gatto L, Fischer B, Pratt B, Egertson J, et al. 2012. A cross-platform toolkit for mass spectrometry and proteomics. *Nat Biotechnol* 30(10): 918-920.

Chen L, Liu L, Qin S, Yang G, Fang K, Zhu B, Kuzyakov Y, Chen P, Xu Y, Yang Y. 2019. Regulation of priming effect by soil organic matter stability over a broad geographic scale. *Nature communications* 10(1): 5112.

Cleary JM, Lipsky ZW, Kim M, Marques CNH, German GK. 2018. Heterogeneous ceramide distributions alter spatially resolved growth of Staphylococcus aureus on human stratum corneum. *J R Soc Interface* 15(141).

Couvillion SP, Danczak RE, Naylor D, Smith ML, Stratton KG, Paurus VL, Bloodsworth KJ, Farris Y, Schmidt DJ, Richardson RE, et al. 2023. Rapid remodeling of the soil lipidome in response to a drying-rewetting event. *Microbiome* 11(1): 34.

da Silva RR, Dorrestein PC, Quinn RA. 2015. Illuminating the dark matter in metabolomics. *Proceedings of the National Academy of Sciences* 112(41): 12549-12550.

de Vries FT, Williams A, Stringer F, Willcocks R, McEwing R, Langridge H, Straathof AL. 2019. Changes in root-exudate-induced respiration reveal a novel mechanism through which drought affects ecosystem carbon cycling. *New Phytol* 224(1): 132-145.

Dietz S, Herz K, Döll S, Haider S, Jandt U, Bruelheide H, Scheel D. 2019. Semi-polar root exudates in natural grassland communities. *Ecology and Evolution* 9(10): 5526-5541.

Djoumbou Feunang Y, Eisner R, Knox C, Chepelev L, Hastings J, Owen G, Fahy E, Steinbeck C, Subramanian S, Bolton E, et al. 2016. ClassyFire: automated chemical classification with a comprehensive, computable taxonomy. *J Cheminform* 8: 61.

Duhrkop K, Fleischauer M, Ludwig M, Aksenov AA, Melnik AV, Meusel M, Dorrestein PC, Rousu J, Bocker S. 2019. SIRIUS 4: a rapid tool for turning tandem mass spectra into metabolite structure information. *Nat Methods* 16(4): 299-302.

Dührkop K, Nothias L-F, Fleischauer M, Reher R, Ludwig M, Hoffmann MA, Petras D, Gerwick WH, Rousu J, Dorrestein PC, et al. 2021. Systematic classification of unknown metabolites using high-resolution fragmentation mass spectra. *Nature Biotechnology* 39(4): 462-471.

Duhrkop K, Nothias LF, Fleischauer M, Reher R, Ludwig M, Hoffmann MA, Petras D, Gerwick WH, Rousu J, Dorrestein PC, et al. 2021. Systematic classification of unknown metabolites using high-resolution fragmentation mass spectra. *Nat Biotechnol* 39(4): 462-471.

Elias KS, Safir GR. 1987. Hyphal Elongation of Glomus fasciculatus in Response to Root Exudates. *Applied and environmental microbiology* 53(8): 1928-1933.

Fan J, Yu L, Xu C. 2017. A Central Role for Triacylglycerol in Membrane Lipid Breakdown, Fatty Acid β-Oxidation, and Plant Survival under Extended Darkness. *Plant Physiol* 174(3): 1517-1530.

Fontaine S, Barot S, Barré P, Bdioui N, Mary B, Rumpel C. 2007. Stability of organic carbon in deep soil layers controlled by fresh carbon supply. *Nature* 450(7167): 277-280.

Glenz R, Kaiping A, Gopfert D, Weber H, Lambour B, Sylvester M, Froschel C, Mueller MJ, Osman M, Waller F. 2022. The major plant sphingolipid long chain base phytosphingosine inhibits growth of bacterial and fungal plant pathogens. *Sci Rep* 12(1): 1081.

Hassan S, Mathesius U. 2012. The role of flavonoids in root-rhizosphere signalling: opportunities and challenges for improving plant-microbe interactions. *J Exp Bot* 63(9): 3429-3444.

Heller SR, McNaught A, Pletnev I, Stein S, Tchekhovskoi D. 2015. InChI, the IUPAC International Chemical Identifier. *J Cheminform* 7: 23.

Heuermann D, Döll S, Schweneker D, Feuerstein U, Gentsch N, von Wirén N. 2023. Distinct metabolite classes in root exudates are indicative for field- or hydroponically-grown cover crops. *Front Plant Sci* 14: 1122285.

Hita C, Parlanti E, Jambu P, Joffre J, Amblès A. 1996. Triglyceride degradation in soil. *Organic Geochemistry* 25(1): 19-28.

Hopkins F, Gonzalez-Meler MA, Flower CE, Lynch DJ, Czimczik C, Tang J, Subke J-A. 2013. Ecosystem-level controls on root-rhizosphere respiration. *New Phytologist* 199(2): 339-351.

Huang AC, Jiang T, Liu Y-X, Bai Y-C, Reed J, Qu B, Goossens A, Nützmann H-W, Bai Y, Osbourn A. 2019. A specialized metabolic network selectively modulates Arabidopsis root microbiota. *Science* 364(6440): eaau6389.

Hugoni M, Luis P, Guyonnet J, Haichar FeZ. 2018. Plant host habitat and root exudates shape fungal diversity. *Mycorrhiza* 28: 451-463.

Jansson JK, Hofmockel KS. 2018. The soil microbiome—from metagenomics to metaphenomics. *Current Opinion in Microbiology* 43: 162-168.

Kallenbach CM, Frey SD, Grandy AS. 2016. Direct evidence for microbial-derived soil organic matter formation and its ecophysiological controls. *Nature communications* 7(1): 13630.

Kameoka H, Gutjahr C. 2022. Functions of Lipids in Development and Reproduction of Arbuscular Mycorrhizal Fungi. *Plant Cell Physiol* 63(10): 1356-1365.

Kolar MJ, Konduri S, Chang T, Wang H, McNerlin C, Ohlsson L, Härröd M, Siegel D, Saghatelian A. 2019. Linoleic acid esters of hydroxy linoleic acids are anti-inflammatory lipids found in plants and mammals. *Journal of Biological Chemistry* 294(27): 10698-10707.

Liang G, Stark J, Waring BG. 2023. Mineral reactivity determines root effects on soil organic carbon. *Nature communications* 14(1): 4962.

Lu Y, Kronzucker HJ, Shi W. 2021. Stigmasterol root exudation arising from Pseudomonas inoculation of the duckweed rhizosphere enhances nitrogen removal from polluted waters. *Environmental Pollution* 287: 117587.

Lu Y, Zhou Y, Nakai S, Hosomi M, Zhang H, Kronzucker HJ, Shi W. 2014. Stimulation of nitrogen removal in the rhizosphere of aquatic duckweed by root exudate components. *Planta* 239(3): 591-603.

Lynch DV, Dunn TM. 2004. An introduction to plant sphingolipids and a review of recent advances in understanding their metabolism and function. *New Phytologist* 161(3): 677-702.

Mark GL, Dow JM, Kiely PD, Higgins H, Haynes J, Baysse C, Abbas A, Foley T, Franks A, Morrissey J, et al. 2005. Transcriptome profiling of bacterial responses to root exudates identifies genes involved in microbe-plant interactions. *Proceedings of the National Academy of Sciences* 102(48): 17454-17459.

Massalha H, Korenblum E, Tholl D, Aharoni A. 2017. Small molecules below-ground: the role of specialized metabolites in the rhizosphere. *Plant J* 90(4): 788-807.

530 McLaughlin S, Zhalnina K, Kosina S, Northen TR, Sasse J. 2023. The core metabolome and root
531 exudation dynamics of three phylogenetically distinct plant species. *Nature communications*
532 14(1): 1649.
533 Monge ME, Dodds JN, Baker ES, Edison AS, Fernández FM. 2019. Challenges in Identifying the
534 Dark Molecules of Life. *Annu Rev Anal Chem (Palo Alto Calif)* 12(1): 177-199.
535 Naasko KI, Naylor D, Graham EB, Couvillion SP, Danczak R, Tolic N, Nicora C, Fransen S, Tao H,
536 Hofmockel KS, et al. 2023. Influence of soil depth, irrigation, and plant genotype on the soil
537 microbiome, metaphenome, and carbon chemistry. *MBio* 14(5): e01758-01723.
538 Naveed M, Brown LK, Raffan AC, George TS, Bengough AG, Roose T, Sinclair I, Koebernick N,
539 Cooper L, Hackett CA, et al. 2017. Plant exudates may stabilize or weaken soil depending on
540 species, origin and time. *European Journal of Soil Science* 68(6): 806-816.
541 Pantigoso HA, Manter DK, Fonte SJ, Vivanco JM. 2023. Root exudate-derived compounds
542 stimulate the phosphorus solubilizing ability of bacteria. *Scientific reports* 13(1): 4050.
543 Peisl BYL, Schymanski EL, Wilmes P. 2018. Dark matter in host-microbiome metabolomics: Tackling
544 the unknowns–A review. *Analytica chimica acta* 1037: 13-27.
545 Peters K, Worrich A, Weinhold A, Alka O, Balcke G, Birkemeyer C, Bruelheide H, Calf OW, Dietz S,
546 Dührkop K, et al. 2018. Current Challenges in Plant Eco-Metabolomics. *International journal of*
547 *molecular sciences* 19(5): 1385.
548 Sasse J, Martinoia E, Northen T. 2018. Feed Your Friends: Do Plant Exudates Shape the Root
549 Microbiome? *Trends in Plant Science* 23(1): 25-41.
550 Schenkel D, Lemfack MC, Piechulla B, Splivallo R. 2015. A meta-analysis approach for assessing
551 the diversity and specificity of belowground root and microbial volatiles. *Front Plant Sci* 6: 707.
552 Schiedung M, Don A, Beare MH, Abiven S. 2023. Soil carbon losses due to priming moderated by
553 adaptation and legacy effects. *Nature Geoscience*.
554 Schmid R, Heuckeroth S, Korf A, Smirnov A, Myers O, Dyrlund TS, Bushuiev R, Murray KJ, Hoffmann
555 N, Lu M, et al. 2023. Integrative analysis of multimodal mass spectrometry data in MZmine 3. *Nat*
556 *Biotechnol* 41(4): 447-449.
557 Schymanski EL, Jeon J, Gulde R, Fenner K, Ruff M, Singer HP, Hollender J. 2014. Identifying Small
558 Molecules via High Resolution Mass Spectrometry: Communicating Confidence. *Environmental*
559 *Science & Technology* 48(4): 2097-2098.
560 Simon L, Haichar FEZ. 2019. Determination of Root Exudate Concentration in the Rhizosphere
561 Using (13)C Labeling. *Bio Protoc* 9(9): e3228.
562 Soliman AH, Radwan SS. 1981. Degradation of Sterols, Triacylglycerol, and Phospholipids by Soil
563 Microorganisms. *Zentralblatt für Bakteriologie, Parasitenkunde, Infektionskrankheiten und*
564 *Hygiene. Zweite Naturwissenschaftliche Abteilung: Mikrobiologie der Landwirtschaft, der*
565 *Technologie und des Umweltschutzes* 136(5): 420-426.
566 Strehmel N, Böttcher C, Schmidt S, Scheel D. 2014. Profiling of secondary metabolites in root
567 exudates of Arabidopsis thaliana. *Phytochemistry* 108: 35-46.
568 Tian B, Pei Y, Huang W, Ding J, Siemann E. 2021. Increasing flavonoid concentrations in root
569 exudates enhance associations between arbuscular mycorrhizal fungi and an invasive plant. *ISME*
570 *J* 15(7): 1919-1930.
571 Van Poecke RM, Posthumus MA, Dicke M. 2001. Herbivore-induced volatile production by
572 Arabidopsis thaliana leads to attraction of the parasitoid Cotesia rubecula: chemical, behavioral,
573 and gene-expression analysis. *J Chem Ecol* 27(10): 1911-1928.

Whalen ED, Grandy AS, Sokol NW, Keiluweit M, Ernakovich J, Smith RG, Frey SD. 2022. Clarifying the evidence for microbial-and plant-derived soil organic matter, and the path toward a more quantitative understanding. *Global Change Biology* 28(24): 7167-7185.

Williams A, Langridge H, Straathof AL, Fox G, Muhammadali H, Hollywood KA, Xu Y, Goodacre R, de Vries FT. 2021. Comparing root exudate collection techniques: An improved hybrid method. *Soil biology & biochemistry* 161: 108391.

Yan S, Yin L, Dijkstra FA, Wang P, Cheng W. 2023. Priming effect on soil carbon decomposition by root exudate surrogates: A meta-analysis. *Soil Biology and Biochemistry* 178: 108955.

Yore MM, Syed I, Moraes-Vieira PM, Zhang T, Herman MA, Homan EA, Patel RT, Lee J, Chen S, Peroni OD, et al. 2014. Discovery of a class of endogenous mammalian lipids with anti-diabetic and anti-inflammatory effects. *Cell* 159(2): 318-332.

Zhalnina K, Louie KB, Hao Z, Mansoori N, da Rocha UN, Shi S, Cho H, Karaoz U, Loqué D, Bowen BP, et al. 2018. Dynamic root exudate chemistry and microbial substrate preferences drive patterns in rhizosphere microbial community assembly. *Nature microbiology* 3(4): 470-480.

Zhang J, Subramanian S, Stacey G, Yu O. 2009. Flavones and flavonols play distinct critical roles during nodulation of Medicago truncatula by Sinorhizobium meliloti. *Plant J* 57(1): 171-183.